

Mesoporous vanadium pentoxide nanofibers with significantly enhanced Li-ion storage properties by electrospinning†

Danmei Yu,^{*ab} Changguo Chen,^b Shuhong Xie,^{cd} Yanyi Liu,^a Kwangsuk Park,^a Xiaoyuan Zhou,^a Qifeng Zhang,^a Jiangyu Li^c and Guozhong Cao^{*ab}

Received 29th July 2010, Accepted 11th November 2010

DOI: 10.1039/c0ee00313a

Mesoporous V_2O_5 nanofibers were fabricated by a method combining sol-gel processing with electrospinning followed by annealing in air. The resultant nanofibers were 350 nm in diameter and consisted of porous polycrystalline vanadium oxide with a specific surface area of $\sim 97 \text{ m}^2 \text{ g}^{-1}$. The mesoporous V_2O_5 nanofibers demonstrated a significantly enhanced Li ion storage capacity of above 370 mA h g^{-1} and a high charge/discharge rate of up to 800 mA g^{-1} with little cyclic degradation.

Vanadium pentoxide, V_2O_5 , which is a typical intercalation compound with a layered crystal structure and a large variety of atomic and molecular species that can be reversibly intercalated and de-intercalated between the layers has been intensively investigated as a cathode material for rechargeable lithium-ion batteries because of its low cost, abundance, easy synthesis, and high energy density since the reversible electrochemical lithium ion intercalation in V_2O_5 was first reported in 1976 by Whittingham.¹ However, the development of rechargeable lithium ion batteries with vanadium pentoxide as a cathode has been limited due to its poor structural stability, low electronic conductivity and ionic conductivity, and slow electrochemical kinetics.^{2,3} In recent years, a lot of research has been focused on the synthesis and fabrication of nanostructured vanadium oxides to mitigate the slow electrochemical kinetics with high specific surface area and short diffusion distance.⁴ It has been demonstrated that single-crystal V_2O_5 nanorod arrays, nanotubes, nanorolls and nanocables possess much improved electrochemical Li-ion interca-

lation properties.⁵⁻⁹ Such an improvement has been attributed to nanostructured materials providing shorter and simpler diffusion paths for lithium ions and allowing the most freedom for dimension change accompanying the lithium ion intercalation and de-intercalation.

There are many methods for fabricating nanomaterials, such as hydrothermal treatment, template-based method, electrodeposition method and so on, but electrospinning is perhaps the most simple and versatile process for generating nanofibers.¹⁰ A variety of simple oxide nanofibers can be readily prepared by electrospinning a polymer solution containing the sol-gel precursors, followed by annealing at a certain temperature.¹¹ Nanofibers with core/sheath, hollow, or porous structures have also been produced by using specially designed spinnerets or adjusting the spinning parameters.¹²⁻¹⁴ Furthermore, single-crystal, polycrystalline, and amorphous V_2O_5 nanofibers have been grown by electrospinning with a poly(vinylpyrrolidone) additive.^{15,16} In this communication, we demonstrated a modified method of fabricating mesoporous vanadium pentoxide nanofibers combining sol-gel processing with electrospinning. It is simple and environmentally benign due to the precursors being prepared directly from V_2O_5 powder and poly(vinylpyrrolidone) (PVP) without using the expensive toxic vanadium oxytriisopropoxide ($VO(OiPr)_3$). The electrochemical characteristics of these nanofibers as cathodes for lithium ion batteries were studied, and the relationship between the microstructure and electrochemical properties were discussed.

Vanadium pentoxide-based fibers with smooth surfaces were prepared by electrospinning from a clear dark red solution containing 1 : 2.5 V_2O_5 sol-gel precursors and PVP (Fig. 1(a)). After annealing at 500°C in air for 1 h, yellowish fibers tens of microns in length were formed (Fig. 1(b)) with an obvious reduction of fiber diameter from $\sim 750 \text{ nm}$ to $\sim 350 \text{ nm}$. Fig. 1(c) demonstrated many pores in the fibers. It was also found that these nanofibers consist of interconnected nano-sized platelet particles of V_2O_5 , as can be seen from Fig. 1(d).

Fig. 2(a) displayed the XRD patterns of V_2O_5 nanofibers before and after annealing at 500°C in air for 1 h, indicating a structural

^aDepartment of Materials Science and Engineering, University of Washington, Seattle, WA, 98195, USA

^bCollege of Chemistry and Chemical Engineering, Chongqing University, Chongqing, 400044, P. R. China

^cDepartment of Mechanical Engineering, University of Washington, Seattle, WA, 98195, USA

^dFaculty of Materials, Optoelectronics and Physics, Xiangtan University, Xiangtan, Hunan, 411105, P. R. China

† Electronic supplementary information (ESI) available: Additional experimental data. See DOI: 10.1039/c0ee00313a

Broader context

In our work, we applied a simple and environmentally benign method for the fabrication of mesoporous vanadium pentoxide nanofibers, combining sol-gel processing with electrospinning, and demonstrated significantly enhanced Li ion intercalation storage capacity, high charge/discharge rate, and excellent cyclic stability. The paper offers new insights for the further development of electrode materials for lithium ion intercalations. And our approach of using electrospinning for the formation of mesoporous vanadium oxide may be applied to a wide range of materials, which may be useful in applications such as catalysis, electrochromics, batteries, and electrochemical capacitors.

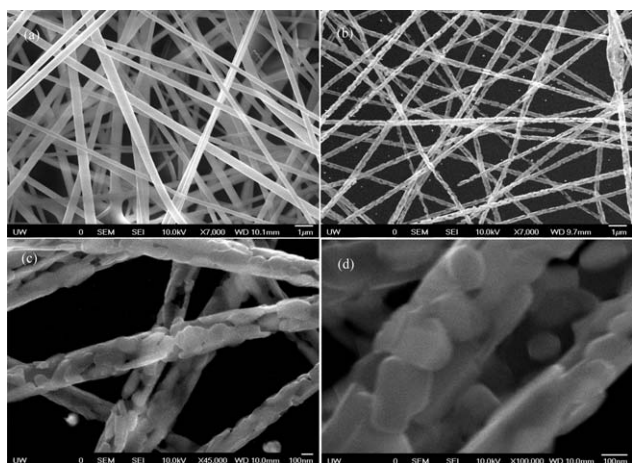


Fig. 1 SEM images of V_2O_5 nanofiber (a) prior to annealing; (b), (c) and (d) after annealing at 500 °C in air for 1 h.

change from hydrous vanadium pentoxide to orthorhombic V_2O_5 . The XRD pattern of as-spun V_2O_5 fibers has a broad $\langle 001 \rangle$ peak, indexed to hydrous vanadium pentoxide as reported in the literature.^{17,18} The fibers treated at 500 °C in air for 1 h showed an XRD pattern of pure orthorhombic V_2O_5 .¹⁷ The interlayer space and grain size of the orthorhombic V_2O_5 were estimated using the Scherrer equation,^{19,20} and was found to be ~ 4.37 Å and ~ 15.5 nm, respectively. Fig. 2(b) depicted the thermogravimetric analysis (TGA) curve of as-spun V_2O_5 fibers. The shape of the TGA curve was similar to those of $V_2O_5 \cdot nH_2O$ xerogels as reported in the literature,¹⁷ suggesting the presence of water and/or residual solvent. The weight change profile for the fibers was characterized by a sharp loss between 350 °C and 470 °C, representing the pyrolysis and/or oxidation of PVP. The weight loss of approximately 50 wt% of nanofibers in

flowing dry air during annealing at 500 °C for 1 h implied the removal of most of the PVP initially added to the precursor colloidal dispersion through oxidation and pyrolysis. However, it is likely that a small amount of carbon is retained in V_2O_5 nanofibers, owing to the incomplete oxidation of PVP. The presence of residual carbon was also suggested by the TGA result of the V_2O_5 fibers annealed at 500 °C in air for 1 h, which showed a further weight loss of 0.3 wt% (see the supporting information, Figure 1S†), and EDS analyses (see the supporting information, Figure 2S†). The presence of such a small amount of carbon may be believed to improve the electrical conductivity of vanadium pentoxide, which was supported by means of electrochemical impedance spectroscopy (EIS) analyses (see the supporting information, Figure 3S†), and consequently benefit the lithium ion intercalation.

Fig. 2(c) showed the typical nitrogen adsorption-desorption isotherm of porous V_2O_5 nanofibers after annealing at 500 °C in air for 1 h, and the pore size distribution calculated from the nitrogen sorption isotherm was also included. The isotherm of porous V_2O_5 nanofibers was a typical IV-type curve with a clear H3-type hysteric loop, which was characteristic of mesoporous materials,^{21,22} suggesting that the V_2O_5 is in the form of non-rigid aggregates of platelet-like particles or assemblages of slit-shaped pores in agreement with the result of SEM.²³ Also, from the nitrogen sorption isotherm, it is calculated that the surface area of these annealed V_2O_5 nanofibers was $97 \text{ m}^2 \text{ g}^{-1}$ and pore volume was 0.2 cc g^{-1} (or 67% porosity). This large surface area was comparable to the surface area of template fabricated mesoporous manganese dioxide, around $91 \text{ m}^2 \text{ g}^{-1}$, and the cathodic-deposited manganese oxide nanowall arrays, $96 \text{ m}^2 \text{ g}^{-1}$.^{21,24} The pore size distribution of mesoporous V_2O_5 nanofibers was centered at 4–5 nm.

Electrochemical properties of the mesoporous vanadium pentoxide nanofibers were investigated systematically as a cathode in lithium ion batteries. Fig. 3(a) and (b) showed typical cyclic

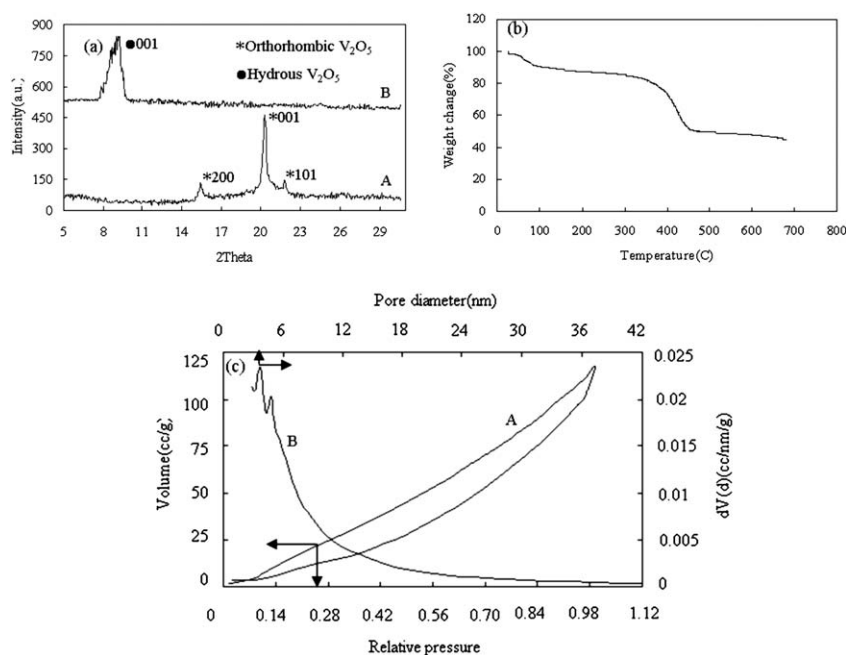


Fig. 2 (a) XRD spectrum of mesoporous V_2O_5 nanofibers; A: after annealing at 500 °C in air for 1 h and B: before annealing; (b) TGA curve of V_2O_5 nanofibers; (c) A: Nitrogen adsorption-desorption isotherm at 77 K of mesoporous V_2O_5 nanofibers; B: pore size distribution of mesoporous V_2O_5 nanofibers.

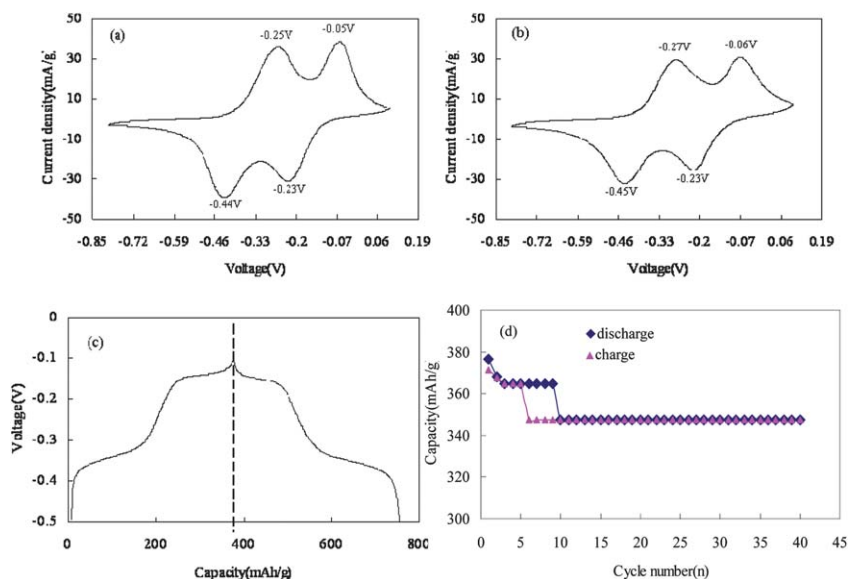


Fig. 3 (a) Cyclic voltammograms of mesoporous V_2O_5 nanofibers in the first cycle and (b) in the 40th cycle with a scan rate of 10 mV s^{-1} in a voltage range between 0.1 V and -0.8 V vs. the Ag/AgCl reference electrode; (c) Chronopotentiometric discharge-charge curves of mesoporous V_2O_5 nanofibers in the 1st cycle with a current density of 625 mA g^{-1} ; (d) The discharge/charge capacity of mesoporous V_2O_5 nanofibers as a function of cyclic numbers.

voltammogram curves of mesoporous V_2O_5 nanofibers using a scan rate of 10 mV s^{-1} . There were two anodic oxidation peaks located at -0.25 V and -0.05 V in the first cycle, which corresponded to Li^+ ion de-intercalation, and cathodic peaks at -0.44 V and -0.23 V , which was attributed to Li^+ intercalation. It has been previously demonstrated that nanorod arrays of V_2O_5 showed cathodic peaks at -0.3 V , -1.1 V and $V_2O_5 \cdot n\text{H}_2\text{O}$ film showed peaks at -0.71 V , 0.12 V under the same condition and using the same reference electrode.^{5,21} This implied that the energy density of lithium ion batteries with the mesoporous V_2O_5 nanofibers cathode should be increased due to the increase of operation voltage, while its reversibility was noticeably improved because there were two pairs of well-defined redox peaks in the CV curves, suggesting no irreversible phase transition. After 41 charge-discharge cycles, the current peak did not decrease dramatically while the voltage difference of redox peaks changed from 0.18 V and 0.17 V in the first cycle to 0.19 V and 0.18 V , respectively, indicating that the mesoporous V_2O_5 nanofibers have excellent cyclic stability and reversibility. Fig. 3(c) depicted CP curves of mesoporous V_2O_5 nanofibers in the 1st cycle in a voltage range between -0.5 V and 0.1 V with a charge/discharge current density of 625 mA g^{-1} . There were two well-defined plateaus in the cathodic and anodic processes from -0.4 V to -0.3 V and -0.2 V to -0.1 V , respectively. The discharge capacity of 377 mA h g^{-1} was delivered in the 1st cycle, much higher than the initial discharge value (140 mA h g^{-1}) of $V_2O_5 \cdot n\text{H}_2\text{O}$ film reported in the literature,^{17,21} while the corresponding charge capacity was found to be 372 mA h g^{-1} with an irreversible capacity of 5.2 mA h g^{-1} . The charge/discharge capacity of mesoporous V_2O_5 nanofibers decreased slowly before the ninth cycle and then the discharge/charge process became very stable (Fig. 3(d)) with a discharge capacity of 347 mA h g^{-1} in the tenth cycle and a loss rate of 0.78% per cycle thereafter until the 40th cycle where the experiment stopped. Although the $V_2O_5 \cdot n\text{H}_2\text{O}$ nanotube arrays, nanocable arrays and nanorod arrays demonstrated higher initial capacity, the capacity of these nanostructured V_2O_5 decreased rapidly during the cyclic test.^{25,26}

Fig. 4 summarizes the lithium ion intercalation capacity of mesoporous V_2O_5 nanofibers at -0.5 V as a function of current density. It can be found that the capacity of Li^+ intercalation in mesoporous vanadium pentoxide nanofibers decreased with the increase of current density, but the change is much less pronounced than that of V_2O_5 nanorods.^{5,8} In other words, the rate performance of mesoporous nanofiber vanadium pentoxide as a cathode in lithium ions batteries was improved greatly. The improved lithium ion intercalation capacity, cyclic stability and reversibility of V_2O_5 nanofibers could be attributed to high surface area, short transport distance, and the presence of a small amount of carbon in the electrode material.

In summary, vanadium pentoxide nanofibers with a mesoporous structure with a specific surface area of $97 \text{ m}^2 \text{ g}^{-1}$ have been prepared by means of electrospinning followed by annealing at $500 \text{ }^\circ\text{C}$ in air. The mesoporous nanofibers consist of orthorhombic V_2O_5 with a small amount of residual carbon, and demonstrated a significantly

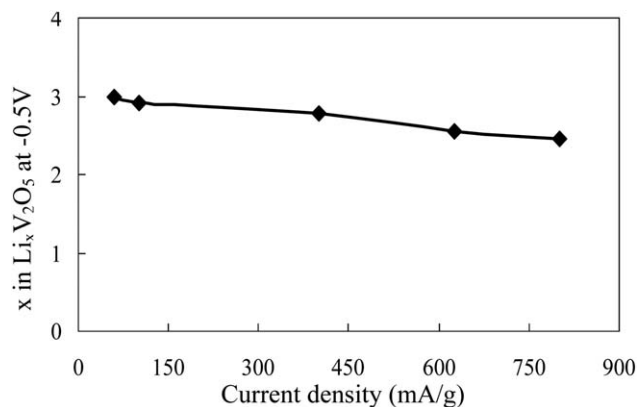


Fig. 4 Relationship between current density and Li^+ intercalation capacity of mesoporous V_2O_5 nanofibers from chronopotentiometric measurements.

enhanced Li-ion storage capacity of $\sim 370 \text{ mA h g}^{-1}$, a high charge/discharge rate of up to 800 mA g^{-1} , and an excellent cyclic stability and reversibility. Such mesoporous V_2O_5 nanofibers allow easy mass and charge transfer with sufficient freedom for volume change accompanying the lithium ion intercalation and de-intercalation.

Experimental section

Vanadium oxide sol was prepared by dissolving 0.146 g V_2O_5 powder (Alfa Aesar) in 4.0 mL 30% H_2O_2 solution at room temperature and stirring vigorously until the V_2O_5 dissolved completely, followed by the addition of 0.359 g of poly(vinylpyrrolidone) (PVP, $M_w \approx 1\,300\,000$) with mixing; a clear dark red solution was obtained in 30 min. This sol preparation method is similar to, but modified from, that reported by Fontenot *et al.*²⁷ In a typical electrospinning experiment, the precursor solution was fed by a syringe pump with a disposable needle of gauge 26 at a rate of 0.15 mL h^{-1} . The metallic needle was connected to a high-voltage power supply (Gamma high voltage research, ES40p-5W) and a piece of Pt foil was placed 15 cm below the tip of the needle to collect the nanofibers at a high-voltage of 15 kV in an electrospinning setup described in detail in the literature.¹⁰ The as-spun nanofiber samples were annealed at 500°C in air for 1 h with a heating rate of $10^\circ\text{C min}^{-1}$. The electrochemical properties of porous V_2O_5 nanofibers were studied using a standard three-electrode system, with 1 M LiClO_4 in propylene carbonate as the electrolyte, a Pt flake as the counter electrode, and Ag/AgCl as the reference electrode. Cyclic voltammetric (CV) tests were carried out between 0.1 and -0.8 V with a scan rate of 10 mV s^{-1} , while the charge-discharge properties of these porous nanofibers were investigated by chronopotentiometric (CP) measurements in the voltages from 0.0 V to -0.5 V with various current densities. Both the CVs and CPs were performed by using an electrochemical analyzer (CH Instruments, Model 605 B). The surface morphology and structure of porous V_2O_5 nanofibers were characterized by means of scanning electron microscopy (SEM, Philips, JEOL JSM7000), X-ray diffraction (XRD, Philips 1820 X-ray diffractometer) and thermogravimetric analysis (TGA7, PerkinElmer). The surface area of these nanofibers were determined by nitrogen adsorption-desorption at 77 K (NOVA 4200e, Brunauer Emmett Teller).

Acknowledgements

This work is supported in part by the National Science Foundation (CMMI 1030048). This research is also supported by the Washington

Research Foundation, National Center for Nanomaterials Technology (Korea), Intel Corporation, and Pacific Northwest National Lab (PNNL). Danmei Yu would like acknowledge the scholarship from the China Scholarship Council.

References

- 1 M. S. Whittingham, *J. Electrochem. Soc.*, 1976, **123**, 315.
- 2 J. X. Wang, C. J. Curtis, D. L. Schulz and J. G. Zhang, *J. Electrochem. Soc.*, 2004, **151**, A1.
- 3 R. Baddour-Hadjean, J. P. Pereira-Ramos, C. Navone and M. Smirnov, *Chem. Mater.*, 2008, **20**, 1916.
- 4 D. W. Liu and G. Z. Cao, *Energy Environ. Sci.*, 2010, **3**, 1218.
- 5 K. Takahashi, S. J. Limmer, Y. Wang and G. Z. Cao, *J. Phys. Chem. B*, 2004, **108**, 9795.
- 6 K. Takahashi, S. J. Limmer, Y. Wang and G. Z. Cao, *Jpn. J. Appl. Phys.*, 2005, **144**, 662.
- 7 N. Li, C. J. Patrissi and C. R. Martin, *J. Electrochem. Soc.*, 2000, **147**, 2044.
- 8 K. Lee, Y. Wang and G. Z. Cao, *J. Phys. Chem. B*, 2005, **109**, 16700.
- 9 Y. Wang and G. Z. Cao, *Adv. Mater.*, 2008, **20**, 2251.
- 10 W. E. Teo and S. Ramakrishna, *Nanotechnology*, 2006, **17**, R89.
- 11 D. Li and Y. N. Xia, *Nano Lett.*, 2003, **3**, 555.
- 12 D. Li and Y. N. Xia, *Nano Lett.*, 2004, **4**, 933.
- 13 J. Yu, S. V. Fridrikh and G. C. Rutledge, *Adv. Mater.*, 2004, **16**, 1562.
- 14 T. Lin, H. Wang and X. Wang, *Adv. Mater.*, 2005, **17**, 2699.
- 15 R. Ostermann, D. Li, Y. Yin, J. T. Mccann and Y. N. Xia, *Nano Lett.*, 2006, **6**, 1297.
- 16 P. Viswanathamurthi, N. Bhattarai, H. Y. Kim and D. R. Lee, *Scr. Mater.*, 2003, **49**, 577.
- 17 Y. Wang, H. M. Shang, T. P. Chou and G. Z. Cao, *J. Phys. Chem. B*, 2005, **109**, 11361.
- 18 V. Petkov, P. N. Trikalitis, E. S. Bozin, S. J. L. Billinge, T. Vogt and M. G. Kanatzidis, *J. Am. Chem. Soc.*, 2002, **124**, 10157.
- 19 G. Z. Cao, *Nanostructures and Nanomaterials, Synthesis Properties and Applications*, Imperial College Press, London, 2004.
- 20 L. S. Birks and H. Friedman, *J. Appl. Phys.*, 1964, **17**, 687.
- 21 D. W. Liu, Y. Y. Liu, B. B. Garcia, Q. F. Zhang, A. Q. Pan, Y. H. Jeong and G. Z. Cao, *J. Mater. Chem.*, 2009, **19**, 8789.
- 22 J. Y. Luo, J. J. Zhang and Y. Y. Xia, *Chem. Mater.*, 2006, **18**, 5618.
- 23 M. Thommes, in *Annual Review of Nano Research*, ed. G. Z. Cao, Q. F. Zhang and C. J. Brinker, World Scientific, Singapore, 2010, vol. 3, ch. 12.
- 24 W. J. Zhou, J. Zhang, T. Xue, D. D. Zhao and H. L. Li, *J. Mater. Chem.*, 2008, **18**, 905.
- 25 K. Takahashi, Y. Wang and G. Z. Cao, *J. Phys. Chem. B*, 2005, **109**, 48.
- 26 Y. Wang and G. Z. Cao, *Chem. Mater.*, 2006, **18**, 2787.
- 27 C. J. Fontenot, J. W. Wiench, M. Pruski and G. L. Schrader, *J. Phys. Chem. B*, 2000, **104**, 11622.